



Published in final edited form as:

Histol Histopathol. 2017 September ; 32(9): 917–928. doi:10.14670/HH-11-856.

Vascular mimicry in glioblastoma following anti-angiogenic and anti-20-HETE therapies

Kartik Angara, Mohammad H. Rashid, Adarsh Shankar, Roxan Ara, Asm Iskander, Thaiz F. Borin, Meenu Jain, Bhagelu R Achyut, and Ali S. Arbab

Laboratory of Tumor Angiogenesis, Georgia Cancer Center, Department of Biochemistry and Molecular Biology, Augusta University, Augusta, GA

Abstract

Glioblastoma (GBM) is one hypervascular and hypoxic tumor known among solid tumors. Antiangiogenic therapeutics (AATs) have been tested as an adjuvant to normalize blood vessels and control abnormal vasculature. Evidence of relapse exemplified in the progressive tumor growth following AAT reflects development of resistance to AATs. Here, we identified that GBM following AAT (Vatalanib) acquired an alternate mechanism to support tumor growth, called vascular mimicry (VM). We observed that Vatalanib induced VM vessels are positive for periodic acid-Schiff (PAS) matrix but devoid of any endothelium on the inner side and lined by tumor cells on the outer-side. The PAS+ matrix is positive for basal laminae (laminin) indicating vascular structures. Vatalanib treated GBM displayed various stages of VM such as initiation (mosaic), sustenance, and full-blown VM. Mature VM structures contain red blood cells (RBC) and bear semblance to the functional blood vessel-like structures, which provide all growth factors to favor tumor growth. Vatalanib treatment significantly increased VM especially in the core of the tumor, where HIF-1 α was highly expressed in tumor cells. VM vessels correlate with hypoxia and are characterized by co-localized MHC-1+ tumor and HIF-1 α expression. Interestingly, 20-HETE synthesis inhibitor HET0016 significantly decreased GBM tumors through decreasing VM structures both at the core and at periphery of the tumors. In summary, AAT induced resistance characterized by VM is an alternative mechanism adopted by tumors to make functional vessels by transdifferentiation of tumor cells into endothelial-like cells to supply nutrients in the event of hypoxia. AAT induced VM is a potential therapeutic target of the novel formulation of HET0016. Our present study suggests that HET0016 has a potential to target therapeutic resistance and can be combined with other antitumor agents in preclinical and clinical trials.

Keywords

Glioblastoma ; Vascular Mimicry ; Angiogenesis ; Vasculogenesis ; Anti-angiogenic therapy ; HET0016; 20-HETE

Introduction

Owing to the hypervascular and hypoxic nature of the glioblastoma (GBM), anti-angiogenic therapies (AATs) have been formulated as an adjuvant to the current standard therapies. The primary motive of the inclusion of AATs in the standard therapies is to inhibit abnormal vasculature and promote the normalization of blood vessels (Los *et al.*, 2007, Dietrich *et al.*, 2008, Norden, Drappatz, *et al.*, 2008b, Norden, Young, *et al.*, 2008). Drugs such as Vatalanib (PTK787), Sunitinib, Cediranib, etc have been used in the clinic with the VEGF-VEGFR signaling pathway being the primary target. However, these drugs offer a transient benefit of a therapeutic response lasting weeks or months. This is followed by an aggressive and higher degree of episodes of relapse, restoration of tumor growth and progression through neovascularization mechanisms (Miller *et al.*, 2005, Norden, Drappatz, *et al.*, 2008b, a, Thompson *et al.*, 2011, Wong *et al.*, 2011, Grabner *et al.*, 2012).

Tumor neovascularization is mediated by critical processes called vasculogenesis and angiogenesis, which establish new blood vessels in the establishing and refractory tumors to promote their growth, invasion, and metastases to distant sites. Vasculogenesis refers to the *de novo* formation of blood vessels following the recruitment and *in situ* differentiation of primitive endothelial progenitors, i.e., angioblasts, into mature endothelial cells that line the blood vessels (Risau & Flamme, 1995). Angiogenesis is defined as the process that gives rise to blood vessels by the proliferation and migration of preexisting, differentiated mature endothelial cells and is a hallmark phenomenon both during embryonic development and postnatal life (Folkman & Shing, 1992, Folkman, 1995, Risau, 1997).

Several studies have demonstrated and conclusively proved that tumor neovascularization is a broad and diverse phenomenon that encompasses numerous additional angiogenic and vasculogenic mechanisms, which include but are not limited to intussusceptive angiogenesis, vessel cooption, vasculogenic mimicry (VM), lymphangiogenesis and recruitment of endothelial progenitor cells (EPCs) to the tumor site (Dome *et al.*, 2007, Hillen & Griffioen, 2007, Folkins *et al.*, 2009, El Hallani *et al.*, 2010, Patenaude *et al.*, 2010, Yu *et al.*, 2010).

Vasculogenic mimicry (VM) is a novel neovascularization phenomenon, which was first reported in melanoma models (Maniotis *et al.*, 1999). Aggressive melanoma cells have the ability to form vasculogenic structures rich in extracellular matrix in tumors capable of carrying functional red blood cells and plasma, and supplying nutrients to the growing tumors. These vessels were devoid of any endothelium but were lined by tumor cells and were positive for Periodic Acid Schiff (PAS) staining (Maniotis *et al.*, 1999). However, our understanding of therapy induced neovascularization is limited and needs preclinical study. Here we report that AAT associated drug resistance and neovascularization is mediated through VM. We used U251 GBM as a model of hypervascular tumor and Vatalanib as a model drug to establish VM. We noticed that hypoxia is critical in VM initiation and formation of functional vessel-like structures in the tumor following Vatalanib treatment. In addition, we have used a novel therapeutic formulation of N-hydroxy-N'-(4-butyl-2-methylphenyl) formamidine (HET0016) for targeting VM. HET0016 is a highly selective inhibitor of 20-hydroxy eicosatetraenoic acid (20-HETE) synthesis by regulating the enzymes of the cytochrome P450 families (Seki *et al.*, 2005) and has been shown to be

involved in inhibiting angiogenesis (Seki *et al.*, 2005, Guo *et al.*, 2007, Guo *et al.*, 2009). Therefore, we hypothesize that tumors develop VM post AAT therapy and HET0016 may potentially inhibit the VM in glioma rat model.

Materials and Methods

Ethics Statement

Animal experiments were performed according to the NIH guidelines and the Institutional Animal Care and Use Committee of the Augusta University (formerly Georgia Regents University) approved the experimental protocol.

Animal model and treatment schedules

Athymic nude rats 6–8 weeks old and weighing 150–170g were randomly separated into different groups of treatment, kept under pathogen-free conditions at room temperature (21–25°C) in 12hr–12hr light dark cycle. Food and water were supplied ad libitum. The rats were purchased from Charles River Laboratory (Frederick, MD, USA) and housed at Augusta University (Augusta, GA, USA). Orthotopic glioma model was created by injecting 4×10^5 human U251 glioma cells suspended in 5 μ L of saline at 3 mm to the right and 1 mm anterior to the bregma as described in our previous publications (Ali *et al.*, 2010, Janic & Arbab, 2012, Kumar *et al.*, 2012).

Animals were randomly assigned to either the drug treatment (Vatalanib, HET0016 (IP or IV) or the control group for the respective treatment regimen (Figure 1). Each treatment group at each time point had at least three animals. Vatalanib (LC Laboratories, Woburn, MA) was prepared for oral administration in 5% DMSO + 20% sucrose water and given once a day at a dose of 50 mg/kg for 2–3 weeks. IP HET0016 (supplied by Dr. John Falck, University of Texas Southwestern) was dissolved with sonication in the cremophor EL/DMSO/PBS (1:1:8 ratio) and was administered by IP route at a dose of 10 mg/kg/day for 2–3 weeks. IV HET0016 was prepared by dissolving HET0016 in DMSO first, then formulated with 30% β -hydroxy-cyclodextrin and administered by intravenous injection (IV) at a dose of 10 mg/kg per day for 2–3 weeks. The control group was treated with the 5% DMSO + 20% sucrose solution by oral gavage for the Vatalanib group, with cremophor EL/DMSO/phosphate-buffered saline (PBS) (in 1:1:8 ratio) by IP for the IP HET0016 group (n=3), with DMSO + 30% β -cyclodextrin by intravenous (IV) for the IV HET0016 group. Drug administration started either on the day of tumor implantation (day 0) and continued for 3 weeks (5 days/week) or 8 days after tumor implantation and continued for two weeks (5 days/week). Twenty-two days after tumor implantation, animals underwent *in vivo* MRI followed by euthanasia and collection of brain tissue.

Histopathology, immunohistochemistry, and PAS staining

Following 2 or 3 wks (3 wks following tumor induction) of treatment, the animals were euthanized and perfused with PBS and 4% paraformaldehyde (Acros Organics, Morris Plains, NJ, USA). Collected brains including tumors were prepared for paraffin blocks and sectioning. Immunohistochemical staining procedures were performed as recommended by the suppliers of primary antibodies. In brief the sections were incubated at 4°C overnight

with the primary antibody (anti-MHC-1; 1:100, Abcam Antibodies, ab#52922) diluted in PBS. Then, the sections were stabilized at room temperature, washed with PBS, and incubated with HRP Polymer Quanto containing the secondary antibody (biotinylated anti-mouse and anti-rabbit immunoglobulins, Ultravision Quanto Detection system HRP kit, Thermo Scientific, TL-060-QHL). The sections were rinsed with PBS/distilled water and incubated with diaminobenzidine tetrachloride (DAB) chromogenic substrate. Following this step, the slides were oxidized in 0.5% Periodic acid solution for 5 min, rinsed in distilled water and incubated with Schiff reagent for 15 min. After this step, the slides were rinsed in lukewarm water and counterstained with hematoxylin, dehydrated, and cover-slipped. To determine the relation of hypoxia and VM, consecutive sections were also double stained with anti-HIF-1 α antibody (R&D systems, MAB1536, 1:100, Proteinase K was used for antigen retrieval) and PAS. To exclude the valid possibility of the contribution of glycogen to PAS staining and thereby discrediting VM, we have also stained these consecutive slides for both laminin and PAS. Laminin stains for the extracellular matrix glycoprotein in the basement membranes of the epithelial, the adjacent and surrounding blood vessel, or vessel like structures and the nerves in the established tissue. The superimposition of the laminin and PAS staining serves to confirm VM and conclusively validates the employment of PAS staining to confirm the same.

Tumor Volume Analysis

Post contrast T1-weighted images were used to determine the tumor volume. Two investigators, blinded to the various treatment groups determined the volume by drawing irregular ROIs (region of interests) for all slices containing tumor. To calculate the exact volume, investigators summed all the slices, and calculated the average area and multiplied by the slice thickness.

Method of identification of vascular mimicry and its different stages

The analysis of the PAS positive areas is extremely tricky. We were interested in investigating the different phases of vascular mimicry, right from its inception, progression, and sustenance. Figures 2 and 3 represent the different phases of vascular mimicry. The host endothelium is remarkably different from vascular mimicry and its different forms, as shown in Figures 2A and 3(i). The PAS staining is superimposed on the small and flattened endothelial nuclei and can be distinguished from the tumor area as it is devoid of the MHC-I staining (human cell marker). Vessel co-option is an adaptive mechanism employed by the tumor to amplify its invasive and metastatic attributes. Tumor cells hijack the existing host endothelial vessels and derive nourishment through the metabolites, oxygen and other nutrients supplied to that particular host tissue vascularized by these vessels. Holash et al (Holash, Maisonpierre, *et al.*, 1999, Holash, Wiegand, *et al.*, 1999) reported the existence of such a phenomenon in the murine models. Fig 2B and 3(ii) show the vessel co-option at the tumor periphery. The existing host endothelium has been hijacked by the tumor as evidenced here by the MHC-I positive staining of the tumor cells co-opting the host blood vessels. We call these vessels '**mosaic vessels (MV)**'. A mosaic vessel perfectly encapsulates the essence of vessel co-option in which both the host endothelial cells and the tumor cells contribute to the PAS staining. Fig 2C and 3(iii) represent the classical new neovascularization phenomenon, which causes marked anti-angiogenic therapy resistance called '**Vascular**

mimicry (VM)'. The blood vessel like structures classified and defined as such have PAS staining contributed exclusively from the tumor cells and are devoid of any host endothelial nuclei. Fig 2D and 3(iv) pictographically demonstrate the sustenance phase of vascular mimicry, which lays the foundation for future vascular mimicry like neovascular structures. This stage of VM is called the '**sustenance of vascular mimicry (SVM)**' and is histologically evident by the PAS positive area of the tumor with increased potential of forming neovascular structures. In areas where such SVM structures are present usually in the shape of a blood vessel, they are devoid of a proper lumen. The tumor cells that contribute to the PAS staining in such structures eventually displace themselves to create the lumen necessary for the formation of such blood vessel like structures.

Quantification of PAS+ vasculatures

From each animal, we have selected one section from each paraffin block-containing tumor (2–3 blocks contained tumors). For analysis, a whole section was imaged using a scanning microscope at 20× magnification and the number of different vessel types determined by two investigators. Any PAS+ areas present either as a complete continuous line or as a complete unconnected dot were considered blood vessel. Based on the inner or outer lining and placement of nucleus, PAS+ structures were divided into four groups as shown in Figures 2 and 3. The first contributed by the host endothelium (HE), the second from the mosaic vessels (MV) formed, the third contributed by the tumor cells, which defines the characteristic vascular mimicry (VM), and the fourth is the sustenance of vascular mimicry (SVM). The number of PAS stained vessels have been counted using the cell counter in the Image J software. The data was analyzed in a way to reflect the results of a treatment group for ease of representation and understanding.

Correlation of tumor Volume, VM and SVM

Tumor volume was calculated as mentioned earlier and subsequently correlated with number of VM.

Statistical analysis

Data were expressed in mean \pm SD unless otherwise stated. Statistical analyses were performed using Student's *t*-test or one-way ANOVA with Bonferroni's post-tests. Any *p* value of less than 0.05 was considered significant. To determine the correlation between the number of VM plus SVM and the volume of the tumor, we performed simple regression analysis for the correlation of tumor volume and VM and SVM.

Results

Increased size of tumors in response to anti-angiogenic therapy

Of all the treatment regimens, we observed that the tumor size was significantly larger in the Vatalanib treated group as shown in Figure 4, which has been confirmed on *in vivo* MRI (Figure 5). The upper panels represent the tumor areas in mice from the D0–21 treatment group and the bottom panel shows the tumor areas from mice in the D8–21 treatment group. The tumor area was defined by staining with MHC-1 (human marker). The large tumors were also found to be extremely hypoxic and had significantly more vascular structures than

the tumors found in the other treatment groups. The images were taken at 0.5× magnification to show the overall size of tumors (highlighted by the dotted red markings) in comparison to the size of the brain (Figure 4). The tumors found in the Vatalanib treated group in the D8–21 group occupied almost half of the hemisphere of the brain. One representative section of one of the animals of each group has been presented here.

VM and SVM following treatment with Vatalanib and HET0016

As indicated in the previous paragraph, Vatalanib treatments caused an increase in tumor size in both treatment groups. Significantly increased tumor size was observed in Day 8–21 Vatalanib treatment group. When PAS+ stained sections were visually compared, there were increased number of PAS+ vascular structures in both groups of Vatalanib treated tumors (Figure 6) compared to that of corresponding control (vehicle treated) tumors. These PAS+ structures were mostly seen in core of the tumors, where HIF-1 α staining is highly positive (Figure 7). We observed strong HIF-1 α immunoreactivity in both nuclei and cytoplasm of the GBM cells in the tumor center as reported in the literature (Kuwai *et al.*, 2003). On the other hand, both groups of HET0016 treated tumors showed smaller tumor sizes as well as a lower number of PAS+ structures both in the core and at the periphery of the tumors compared to that of control and Vatalanib treated groups (Figure 6). Compared to the control and Vatalanib treated tumors, tumor core also showed lesser HIF-1 α positive areas. To confirm that these PAS+ areas are not due to deposition of glycogen secreted from metabolically active tumor cells, we also stained for vascular basal laminae (laminin). Figure 8 shows the superimposition of PAS+ areas with that of laminin indicating PAS+ vascular structures and not merely glycogen deposition.

We considered both VM and SVM as tumor cell derived vessels and compared the total number of the structures among the groups of tumors. Quantitative analysis indicated a significantly higher number of VM plus SVM in both groups of Vatalanib treatments compared to that of corresponding control and HET0016 groups (Figure 9). IV HET 8–21 group showed a significantly lower number of VM plus SVM compared to that of corresponding control and Vatalanib treated groups. Although significant difference in reduction of VM and SVM was not achieved in both day 0–21 and day 8–21 IP HET0016 groups as well as days 0–21 IV HET0016, the latter group showed a lower number of VM plus SVM in the tumors. These findings were also confirmed by the representative PAS and MHC-1 stained sections (Figure 6).

Increased tumor size correlates with increased incidence of Vascular Mimicry

We hypothesized that larger tumor (whether treated or non-treated) will be more hypoxic and there will be more VM or SVM. We performed simple regression analysis and correlated tumor volume with total VM (VM plus SVM). We observed that an increase in tumor volume positively correlated with increased incidence of VM ($p=0.001$) (Figure 9). We noted that in tumors with larger volume, especially in the center, where the tumor is primarily hypoxic, VM plays a crucial role in initiating neovascularization. Its sustenance can also be seen in the center but not in the periphery.

Discussion

Glioblastomas are extremely hypervascular tumors with high incidence of relapse and notorious refractoriness. Because of these attributes, it is extremely difficult to treat these tumors (Stupp *et al.*, 2005). Anti angiogenic therapy (AAT) has been formulated as an adjuvant to the standard treatment modules (Chinot & Reardon, 2014). However, the transient benefits offered by this therapy and the subsequent pathological hypervascularity observed in these tumors necessitated the study of these neovascularization mechanisms in tumors in response to therapy. Vatalanib targets the VEGF-VEGFR2 pathway to inhibit classical angiogenesis (Mross *et al.*, 2005). The increasing incidences of relapses of tumor and the subsequent progressive tumor growth point towards the development of resistance of tumors to AAT (Miller *et al.*, 2005, Norden, Drappatz, *et al.*, 2008b, a, Norden, Young, *et al.*, 2008, Thompson *et al.*, 2011, Wong & Brem, 2011, Wong *et al.*, 2011, Grabner *et al.*, 2012). The initiation of alternative signaling pathways such as the basic fibroblast growth factor (bFGF), IL8-CXCR1-CXCR2, Tie-2, stromal-cell derived factor-1 α (SDF-1 α), and increased VEGF production leading to hypervascularity and increased invasiveness of the tumor cells are some of the important explanations for the development of resistance of tumors to AAT (Batchelor *et al.*, 2007, Kerbel, 2008, Norden, Drappatz, *et al.*, 2008b). Hypoxia results in the upregulation of HIF-1 α . HIF-1 α induces the production of a potent chemoattractant called the stromal derived factor 1-alpha (SDF-1 α), which serves to promote the recruitment, migration and accumulation of bone marrow derived cells (BMDCs) to the TME by signaling through the CXCR4 receptors on the surface of BMDCs. These BMDCs include cells such as endothelial progenitor cells (EPCs), angiogenic monocytes, tumor associated macrophages, and MDSCs (Zhang *et al.*, 2002, Arbab *et al.*, 2008, Du *et al.*, 2008, Achyut *et al.*, 2015, Achyut & Arbab, 2016, Achyut *et al.*, 2016). These are classical players that serve to provide an explanation of vasculogenesis. However, in recent years our groups and other investigators have noticed vessel like structures that are formed by tumor cells in GBM following AAT. These tumor cell derived vessel like structures are called VM (Arbab *et al.*, 2015).

The primary motive of the inclusion of AATs in the standard therapies is to inhibit abnormal neovascularization and promote the normalization of blood vessels (Los *et al.*, 2007, Dietrich *et al.*, 2008, Norden, Drappatz, *et al.*, 2008b, Norden, Young, *et al.*, 2008). Drugs such as Vatalanib (PTK787), Sunitinib, Cediranib, etc have been used in the clinic with the VEGF-VEGFR signaling pathway being the primary target. However, these drugs offer a transient benefit of a therapeutic response lasting weeks or months. This is followed by a more aggressive comeback by tumors as reflected in the higher degree of episodes of relapse, restoration of tumor growth and progression (Miller *et al.*, 2005, Norden, Drappatz, *et al.*, 2008b, a, Thompson *et al.*, 2011, Wong *et al.*, 2011, Grabner *et al.*, 2012). However, there has been no study demonstrating AAT induced VM in tumors. Previous studies have demonstrated the presence of VM and mosaic vessels composed of endothelial cells, tumor cells and basement membrane crucial to the invasion of tumor and immunohistologically representing vessel co-option in tumors (Liu *et al.*, 2011). Another study demonstrated the presence of PAS-positive networks and closed loops within the tumor in which each loop surrounded nests or smaller lobules of glioblastoma tumor cells, characteristic of VM (Chen

et al., 2012). Vascular Mimicry is a pathological neovascularization mechanism adopted by tumors to counter the drastic effects exhibited by the Anti-angiogenic and other chemotherapeutic strategies. VM structures are rich in extracellular patterned matrices abundant in laminin, heparan sulfate, proteoglycan, and collagens IV and VI (Maniotis *et al.*, 1999, Folberg & Maniotis, 2004). For the tumor cells to meet with their growing metabolic, nutrient and oxygen demands, it is imperative that metastasis is a viable option. The process of neovascularization is indispensable for metastases to happen. The formation of patterned matrices has already been conclusively established as crucial histopathological evidence for VM and corroborated in our current study as well. These patterned matrices capable of forming vascular networks are composed of a basement membrane made of glycoproteins and heparan sulfate that are visualized by PAS staining as well as laminin (Folberg *et al.*, 1993, Chen *et al.*, 2002, Clarijs *et al.*, 2002). In the present study, we have stained consecutive sections with laminin and PAS. We have noticed that in most of the areas in the tumor, the PAS staining superimposed on the laminin staining, thereby ruling out the possibility that the PAS staining was the contribution of the excess glycogen deposits generated by hypoxia. We have also observed PAS in areas negative for laminin. We believe that the basement membrane required for the lumen formation capable of generating vascular structures carrying plasma and functional Red Blood Cells (RBCs) would be an eventual step in VM formation and this could be the reason why we do not see laminin staining in areas where PAS staining is present by itself. Our laminin-PAS co-staining therefore strongly negates the possibility of the hypoxia-mediated glycogen deposit and further conclusively proves VM in our model. Our studies have also corroborated the same evidence demonstrated by the above mentioned investigations in tumors (Folberg *et al.*, 1993, Chen *et al.*, 2002, Clarijs *et al.*, 2002). We report for the first time the presence of such neovascular structures and establish the existence of such structures as an adaptive mechanism of tumor cells to meet with their growing demand of nutrient, oxygen and metabolic supply following AAT. The presence of higher expression of HIF-1 α at the core of AAT treated GBM also indicates hypoxia following AAT and suggests that hypoxia may have contributed to more VM. Moreover, AAT may have caused alternative neovascularization and refractory growth of GBM causing further hypoxia and development of more VM.

Our results showed that the increased size of the tumors positively correlated with the increased incidence of VM in the hypoxic tumor core. Our data suggest that hypoxia drives the VM and its sustenance in the tumor center to generate new blood vessels. We found higher expression of HIF-1 α , both nuclear and cytoplasmic, at core of AAT treated tumor indicating hypoxia which may have contributed to accelerating VM. Moreover, these blood vessels help the tumors to grow and meet the metabolic and nutrient supply for invasion and metastasis. One of the most crucial steps in the VM is the transdifferentiation of mature GBM cells into glioblastoma stem like cells (GSCs) with endothelial properties. Several studies have already established that tumor cells transdifferentiate into endothelial like cells (termed tumor derived endothelial cells, TDECs), which were CD45 negative but CD31 and CD34 positive, and GSC with CD133+CD144+ phenotype promote the VM in GBM tumors (Soda *et al.*, 2011). Previous studies have also reported the presence of endothelial progenitor like characteristics of CD133+ glioma stem like cells or glioma initiating cells. We suspect that

the hypoxic conditions in the tumors promote VM and its sustenance by the generation of these GSCs. In addition, CD144 (VE-Cadherin), which is also regulated by hypoxia, has been cited as the key molecule driving VM in GBM (Chiao *et al.*, 2011, Mao *et al.*, 2013).

In the current study, we used a novel therapeutic IV formulation of N-hydroxy-N'-(4-butyl-2-methylphenyl) formamidine (HET0016), a highly selective inhibitor of 20-hydroxy arachidonic acid (20-HETE) synthesis by targeting the enzymes of the cytochrome P450, family 4, subfamily A (CYP4A) and CYP4F families (Seki *et al.*, 2005). 20-HETE induces the angiogenic responses in endothelial cells by stimulating the production of VEGF and HIF-1 α . These factors are crucial for the induction of such angiogenic responses (Guo *et al.*, 2007, Guo *et al.*, 2009). HET0016 effectively controls the angiogenic responses induced by several growth factors, cytokines and chemokines, and was also shown to inhibit tumor growth induced by implanted human U251 cells, gliosarcoma and other tumors (Chen *et al.*, 2005, Guo *et al.*, 2006, Borin *et al.*, 2014, Shankar *et al.*, 2016). HET0016 administered through IP or IV route showed decreased formation of VM compared to that of Vatalanib treated animals in our studies. For IV formulation, we have used β -hydroxy-cyclodextrin as delivery vehicle for enhanced delivery to the hypervascular GBM by exploiting enhanced permeability and retention (EPR) effects. Our ongoing studies showed increased uptake and retention of IV formulated HET0016 in GBM compared to IP formulated HET0016 and caused significant inhibition of tumor growth and vascularization (data not shown). However, most strikingly, a significantly lower number of VM was observed in animals that were treated with HET0016 IV from day 8 of tumor implantation, which could be due to the effect of higher concentration of HET0016 on the tumor cells as well as endothelial cells in and around the tumor as shown in our previous studies (Ali *et al.*, 2010). Our previous studies also indicated lower expression of HIF-1 α in tumors following HET0016 (Borin *et al.*, 2014). Our ongoing studies focus on discovering novel pathways involved in preventing VM by HET0016.

In summary, our study suggests that AAT associated drug resistance and neovascularization is mediated through VM. Hypoxia is critical in VM initiation and formation of functional vessel-like structures in the tumor following vatalanib treatment. In addition, we employed the use of a novel therapeutic formulation of HET0016 for targeting VM. HET0016 could be an alternative agent to target tumor growth as well as formation of neovascularization including VM.

References

- Achyut BR, Arbab AS. Myeloid cell signatures in tumor microenvironment predicts therapeutic response in cancer. *OncoTargets and therapy*. 2016; 9:1047–1055. [PubMed: 27042097]
- Achyut BR, Shankar A, Iskander AS, Ara R, Knight RA, Scicli AG, Arbab AS. Chimeric mouse model to track the migration of bone marrow derived cells in glioblastoma following anti-angiogenic treatments. *Cancer biology & therapy*. 2016; 17:280–290. [PubMed: 26797476]
- Achyut BR, Shankar A, Iskander AS, Ara R, Angara K, Zeng P, Knight RA, Scicli AG, Arbab AS. Bone marrow derived myeloid cells orchestrate antiangiogenic resistance in glioblastoma through coordinated molecular networks. *Cancer letters*. 2015; 369:416–426. [PubMed: 26404753]
- Ali MM, Janic B, Babajani-Feremi A, Varma NR, Iskander AS, Anagli J, Arbab AS. Changes in vascular permeability and expression of different angiogenic factors following anti-angiogenic treatment in rat glioma. *PLoS ONE*. 2010; 5:e8727. [PubMed: 20090952]

- Arbab AS, Jain M, Achyut BR. Vascular mimicry: The next big glioblastoma target. *Biochemistry & physiology*. 2015; 4
- Arbab AS, Janic B, Knight RA, Anderson SA, Pawelczyk E, Rad AM, Read EJ, Pandit SD, Frank JA. Detection of migration of locally implanted ac133+ stem cells by cellular magnetic resonance imaging with histological findings. *FASEB J*. 2008; 22:3234–3246. [PubMed: 18556461]
- Batchelor TT, Sorensen AG, di Tomaso E, Zhang WT, Duda DG, Cohen KS, Kozak KR, Cahill DP, Chen PJ, Zhu M, Ancukiewicz M, Mrugala MM, Plotkin S, Drappatz J, Louis DN, Ivy P, Scadden DT, Benner T, Loeffler JS, Wen PY, Jain RK. Aza2171, a pan-vegfr tyrosine kinase inhibitor, normalizes tumor vasculature and alleviates edema in glioblastoma patients. *Cancer Cell*. 2007; 11:83–95. [PubMed: 17222792]
- Borin TF, Zuccari DA, Jardim-Perassi BV, Ferreira LC, Iskander AS, Varma NR, Shankar A, Guo AM, Scicli G, Arbab AS. Het0016, a selective inhibitor of HIF-1 synthesis, decreases pro-angiogenic factors and inhibits growth of triple negative breast cancer in mice. *PLoS One*. 2014; 9:e116247. [PubMed: 25549350]
- Chen P, Guo M, Wylie D, Edwards PA, Falck JR, Roman RJ, Scicli AG. Inhibitors of cytochrome p450 4a suppress angiogenic responses. *Am J Pathol*. 2005; 166:615–624. [PubMed: 15681843]
- Chen X, Maniotis AJ, Majumdar D, Pe'er J, Folberg R. Uveal melanoma cell staining for cd34 and assessment of tumor vascularity. *Investigative ophthalmology & visual science*. 2002; 43:2533–2539. [PubMed: 12147581]
- Chen Y, Jing Z, Luo C, Zhuang M, Xia J, Chen Z, Wang Y. Vasculogenic mimicry-potential target for glioblastoma therapy: An in vitro and in vivo study. *Med Oncol*. 2012; 29:324–331. [PubMed: 21161444]
- Chiao MT, Yang YC, Cheng WY, Shen CC, Ko JL. Cd133+ glioblastoma stem-like cells induce vascular mimicry in vivo. *Current neurovascular research*. 2011; 8:210–219. [PubMed: 21675958]
- Chinot OL, Reardon DA. The future of antiangiogenic treatment in glioblastoma. *Curr Opin Neurol*. 2014; 27:675–682. [PubMed: 25313693]
- Clarijs R, Otte-Holler I, Ruiters DJ, de Waal RM. Presence of a fluid-conducting meshwork in xenografted cutaneous and primary human uveal melanoma. *Investigative ophthalmology & visual science*. 2002; 43:912–918. [PubMed: 11923228]
- Dietrich J, Norden AD, Wen PY. Emerging antiangiogenic treatments for gliomas - efficacy and safety issues. *Curr Opin Neurol*. 2008; 21:736–744. [PubMed: 19060566]
- Dome B, Hendrix MJC, Paku S, Tovari J, Timar J. Alternative vascularization mechanisms in cancer: Pathology and therapeutic implications. *Am J Pathol*. 2007; 170:1–15. [PubMed: 17200177]
- Du R, Lu KV, Petritsch C, Liu P, Ganss R, Passegue E, Song H, Vandenberg S, Johnson RS, Werb Z, Bergers G. Hif1alpha induces the recruitment of bone marrow-derived vascular modulatory cells to regulate tumor angiogenesis and invasion. *Cancer Cell*. 2008; 13:206–220. [PubMed: 18328425]
- El Hallani S, Boisselier B, Peglion F, Rousseau A, Colin C, Idbah A, Marie Y, Mokhtari K, Thomas J-L, Eichmann A, Delattre J-Y, Maniotis AJ, Sanson M. A new alternative mechanism in glioblastoma vascularization: Tubular vasculogenic mimicry. *Brain*. 2010; 133:973–982. [PubMed: 20375132]
- Folberg R, Maniotis AJ. Vasculogenic mimicry. *APMIS*. 2004; 112:508–525. [PubMed: 15563313]
- Folberg R, Rummelt V, Parys-Van Ginderdeuren R, Hwang T, Woolson RF, Pe'er J, Gruman LM. The prognostic value of tumor blood vessel morphology in primary uveal melanoma. *Ophthalmology*. 1993; 100:1389–1398. [PubMed: 8371929]
- Folkins C, Shaked Y, Man S, Tang T, Lee CR, Zhu Z, Hoffman RM, Kerbel RS. Glioma tumor stem-like cells promote tumor angiogenesis and vasculogenesis via vascular endothelial growth factor and stromal-derived factor 1. *Cancer Res*. 2009; 69:7243–7251. [PubMed: 19738068]
- Folkman J. Clinical applications of research on angiogenesis. *N Engl J Med*. 1995; 333:1757–1763. [PubMed: 7491141]
- Folkman J, Shing Y. Angiogenesis. *Journal of Biological Chemistry*. 1992; 267:10931–10934. [PubMed: 1375931]
- Grabner G, Nobauer I, Elandt K, Kronnerwetter C, Woehrer A, Marosi C, Prayer D, Trattnig S, Preusser M. Longitudinal brain imaging of five malignant glioma patients treated with

bevacizumab using susceptibility-weighted magnetic resonance imaging at 7 t. *Magn Reson Imaging*. 2012; 30:139–147. [PubMed: 21982163]

- Guo AM, Scicli G, Sheng J, Falck JC, Edwards PA, Scicli AG. 20-hete can act as a nonhypoxic regulator of hif-1{alpha} in human microvascular endothelial cells. *Am J Physiol Heart Circ Physiol*. 2009; 297:H602–H613. [PubMed: 19502554]
- Guo AM, Arbab AS, Falck JR, Chen P, Edwards PA, Roman RJ, Scicli AG. Activation of vascular endothelial growth factor through reactive oxygen species mediates 20-hydroxyeicosatetraenoic acid-induced endothelial cell proliferation. *J Pharmacol Exp Ther*. 2007; 321:18–27. [PubMed: 17210799]
- Guo M, Roman RJ, Fenstermacher JD, Brown SL, Falck JR, Arbab AS, Edwards PA, Scicli AG. 9l gliosarcoma cell proliferation and tumor growth in rats are suppressed by n-hydroxy-n'-(4-butyl-2-methylphenol) formamidine (het0016), a selective inhibitor of cyp4a. *J Pharmacol Exp Ther*. 2006; 317:97–108. [PubMed: 16352703]
- Hillen F, Griffioen A. Tumour vascularization: Sprouting angiogenesis and beyond. *Cancer and Metastasis Reviews*. 2007; 26:489–502. [PubMed: 17717633]
- Holash J, Wiegand SJ, Yancopoulos GD. New model of tumor angiogenesis: Dynamic balance between vessel regression and growth mediated by angiopoietins and vegf. *Oncogene*. 1999; 18:5356–5362. [PubMed: 10498889]
- Holash J, Maisonpierre PC, Compton D, Boland P, Alexander CR, Zagzag D, Yancopoulos GD, Wiegand SJ. Vessel cooption, regression, and growth in tumors mediated by angiopoietins and vegf. *Science*. 1999; 284:1994–1998. [PubMed: 10373119]
- Janic B, Arbab AS. Cord blood endothelial progenitor cells as therapeutic and imaging probes. *Imaging Med*. 2012; 4:477–490. [PubMed: 23227114]
- Kerbel RS. Tumor angiogenesis. *N Engl J Med*. 2008; 358:2039–2049. [PubMed: 18463380]
- Kumar S, Arbab AS, Jain R, Kim J, Decarvalho AC, Shankar A, Mikkelsen T, Brown SL. Development of a novel animal model to differentiate radiation necrosis from tumor recurrence. *J Neurooncol*. 2012
- Kuwai T, Kitadai Y, Tanaka S, Onogawa S, Matsutani N, Kaio E, Ito M, Chayama K. Expression of hypoxia-inducible factor-1alpha is associated with tumor vascularization in human colorectal carcinoma. *International journal of cancer*. 2003; 105:176–181. [PubMed: 12673675]
- Liu Z, Li Y, Zhao W, Ma Y, Yang X. Demonstration of vasculogenic mimicry in astrocytomas and effects of endostar on u251 cells. *Pathology, research and practice*. 2011; 207:645–651.
- Los M, Roodhart JM, Voest EE. Target practice: Lessons from phase iii trials with bevacizumab and vatalanib in the treatment of advanced colorectal cancer. *Oncologist*. 2007; 12:443–450. [PubMed: 17470687]
- Maniotis AJ, Folberg R, Hess A, Seftor EA, Gardner LM, Pe'er J, Trent JM, Meltzer PS, Hendrix MJ. Vascular channel formation by human melanoma cells in vivo and in vitro: Vasculogenic mimicry. *Am J Pathol*. 1999; 155:739–752. [PubMed: 10487832]
- Mao XG, Xue XY, Wang L, Zhang X, Yan M, Tu YY, Lin W, Jiang XF, Ren HG, Zhang W, Song SJ. Cdh5 is specifically activated in glioblastoma stemlike cells and contributes to vasculogenic mimicry induced by hypoxia. *Neuro-oncology*. 2013; 15:865–879. [PubMed: 23645533]
- Miller KD, Sweeney CJ, Sledge GW Jr. Can tumor angiogenesis be inhibited without resistance? *EXS*. 2005:95–112. [PubMed: 15617473]
- Mross K, Drevs J, Muller M, Medinger M, Marme D, Hennig J, Morgan B, Lebwohl D, Masson E, Ho YY, Gunther C, Laurent D, Unger C. Phase i clinical and pharmacokinetic study of ptk/zk, a multiple vegf receptor inhibitor, in patients with liver metastases from solid tumours. *Eur J Cancer*. 2005; 41:1291–1299. [PubMed: 15939265]
- Norden AD, Drappatz J, Wen PY. Antiangiogenic therapy in malignant gliomas. *Curr Opin Oncol*. 2008a; 20:652–661. [PubMed: 18841047]
- Norden AD, Drappatz J, Wen PY. Novel anti-angiogenic therapies for malignant gliomas. *Lancet Neurol*. 2008b; 7:1152–1160. [PubMed: 19007739]
- Norden AD, Young GS, Setayesh K, Muzikansky A, Klufas R, Ross GL, Ciampa AS, Ebbeling LG, Levy B, Drappatz J, Kesari S, Wen PY. Bevacizumab for recurrent malignant gliomas: Efficacy, toxicity, and patterns of recurrence. *Neurology*. 2008; 70:779–787. [PubMed: 18316689]

- Patenaude A, Parker J, Karsan A. Involvement of endothelial progenitor cells in tumor vascularization. *Microvascular Research*. 2010; 79:217–223. [PubMed: 20085777]
- Risau W. Mechanisms of angiogenesis. *Nature*. 1997; 386:671–674. [PubMed: 9109485]
- Risau W, Flamme I. Vasculogenesis. *Annual Review of Cell and Developmental Biology*. 1995; 11:73–91.
- Seki T, Wang MH, Miyata N, Laniado-Schwartzman M. Cytochrome p450 4a isoform inhibitory profile of n-hydroxy-n'-(4-butyl-2-methylphenyl)-formamidine (het0016), a selective inhibitor of 20-hete synthesis. *Biol Pharm Bull*. 2005; 28:1651–1654. [PubMed: 16141533]
- Shankar A, Borin TF, Iskander A, Varma NR, Achyut BR, Jain M, Mikkelsen T, Guo AM, Chwang WB, Ewing JR, Bagher-Ebadian H, Arbab AS. Combination of vatalanib and a 20-hete synthesis inhibitor results in decreased tumor growth in an animal model of human glioma. *OncoTargets and therapy*. 2016; 9:1205–1219. [PubMed: 27022280]
- Soda Y, Marumoto T, Friedmann-Morvinski D, Soda M, Liu F, Michiue H, Pastorino S, Yang M, Hoffman RM, Kesari S, Verma IM. Transdifferentiation of glioblastoma cells into vascular endothelial cells. *Proc Natl Acad Sci U S A*. 2011; 108:4274–4280. [PubMed: 21262804]
- Stupp R, Mason WP, van den Bent MJ, Weller M, Fisher B, Taphoorn MJ, Belanger K, Brandes AA, Marosi C, Bogdahn U, Curschmann J, Janzer RC, Ludwin SK, Gorlia T, Allgeier A, Lacombe D, Cairncross JG, Eisenhauer E, Mirimanoff RO. European Organisation for R., Treatment of Cancer Brain T., Radiotherapy G. and National Cancer Institute of Canada Clinical Trials G. Radiotherapy plus concomitant and adjuvant temozolomide for glioblastoma. *N Engl J Med*. 2005; 352:987–996. [PubMed: 15758009]
- Thompson EM, Frenkel EP, Neuwelt EA. The paradoxical effect of bevacizumab in the therapy of malignant gliomas. *Neurology*. 2011; 76:87–93. [PubMed: 21205697]
- Wong ET, Brem S. Taming glioblastoma by targeting angiogenesis: 3 years later. *J Clin Oncol*. 2011; 29:124–126. [PubMed: 21135277]
- Wong ET, Gautam S, Malchow C, Lun M, Pan E, Brem S. Bevacizumab for recurrent glioblastoma multiforme: A meta-analysis. *J Natl Compr Canc Netw*. 2011; 9:403–407. [PubMed: 21464145]
- Yu L, Su B, Hollomon M, Deng Y, Facchinetti V, Kleinerman ES. Vasculogenesis driven by bone marrow-derived cells is essential for growth of ewing's sarcomas. *Cancer Res*. 2010; 70:1334–1343. [PubMed: 20124484]
- Zhang ZG, Zhang L, Jiang Q, Chopp M. Bone marrow-derived endothelial progenitor cells participate in cerebral neovascularization after focal cerebral ischemia in the adult mouse. *Circulation Research*. 2002; 90:284–288. [PubMed: 11861416]

Treatment schedules in rats

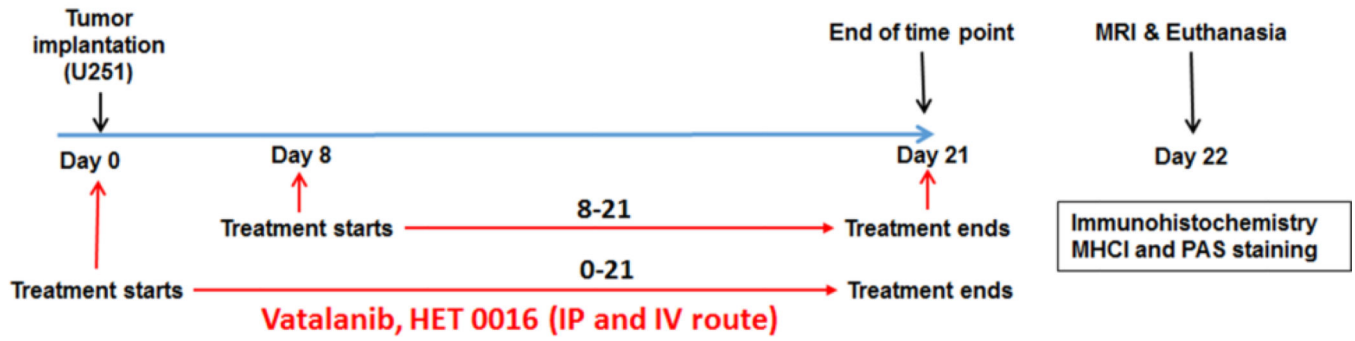


Figure 1. Schematic shows orthotopic tumor implantation, schedules of treatments and end of tumor studies.

Author Manuscript

Author Manuscript

Author Manuscript

Author Manuscript

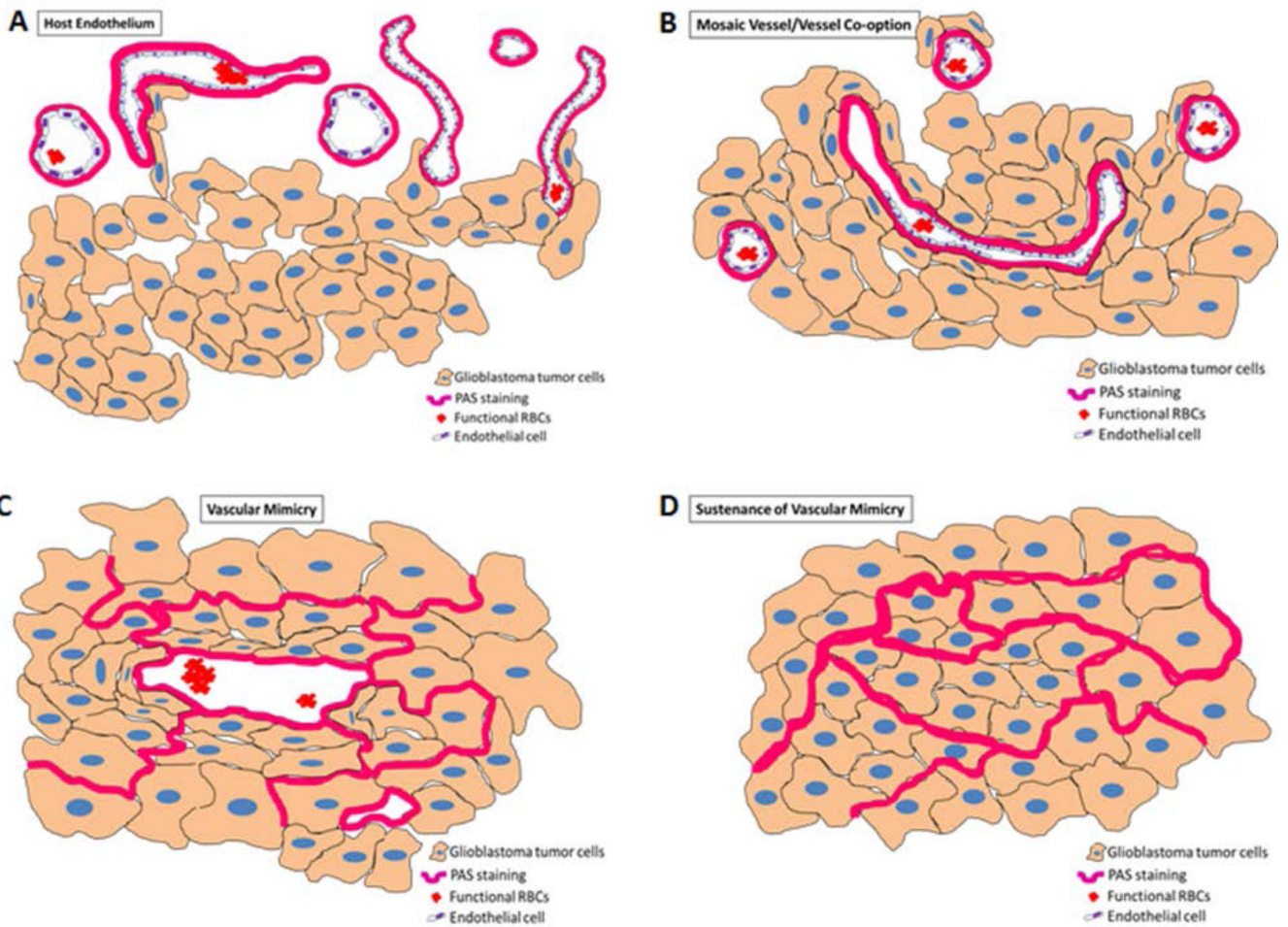


Figure 2. Models showing vessel heterogeneity and VM in GBM tumor
 These models were used to determine the number of VM in the tumors.

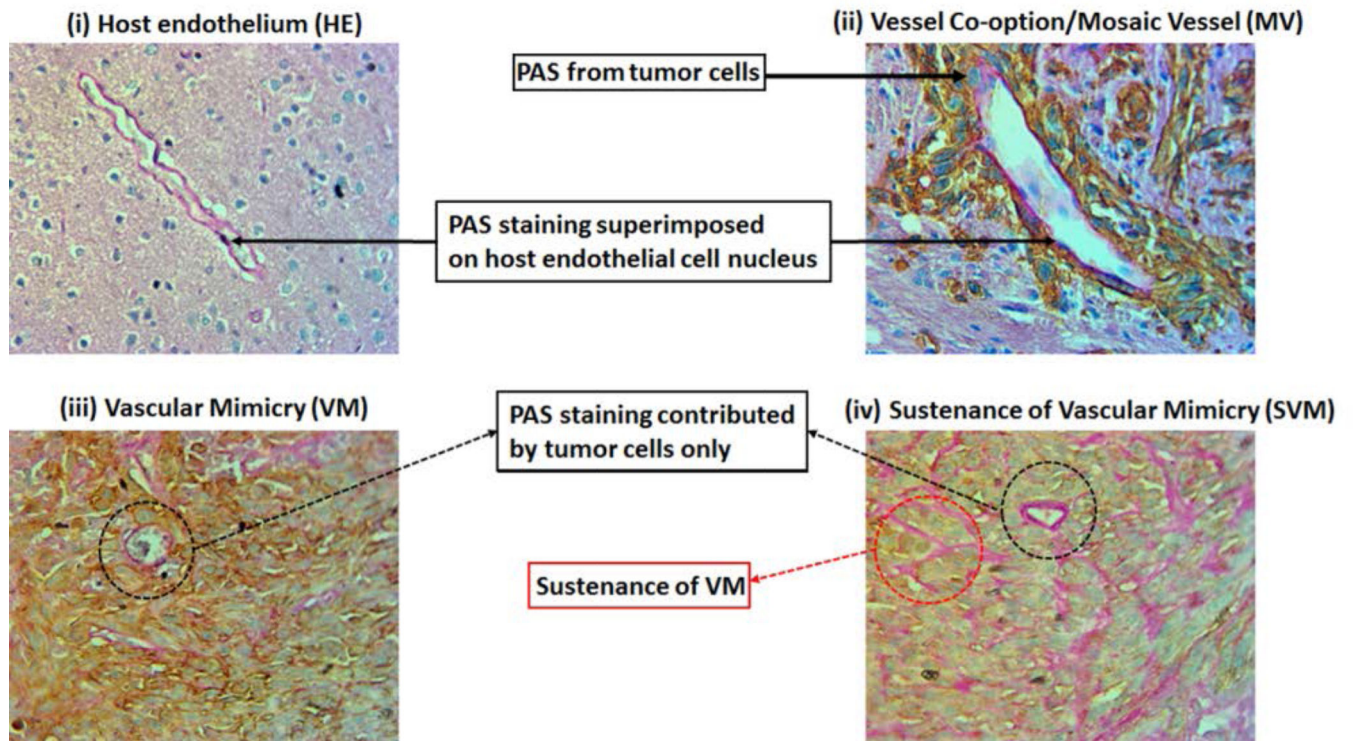


Figure 3. Evidence of AAT induced VM and its different stages in GBM tumor growth
 (A) IHC images showing PAS staining representing (i) host endothelium (HE), (ii) mosaic vessel (MV), (iii) vascular mimicry (VM) and (iv) sustenance of vascular mimicry (SVM).

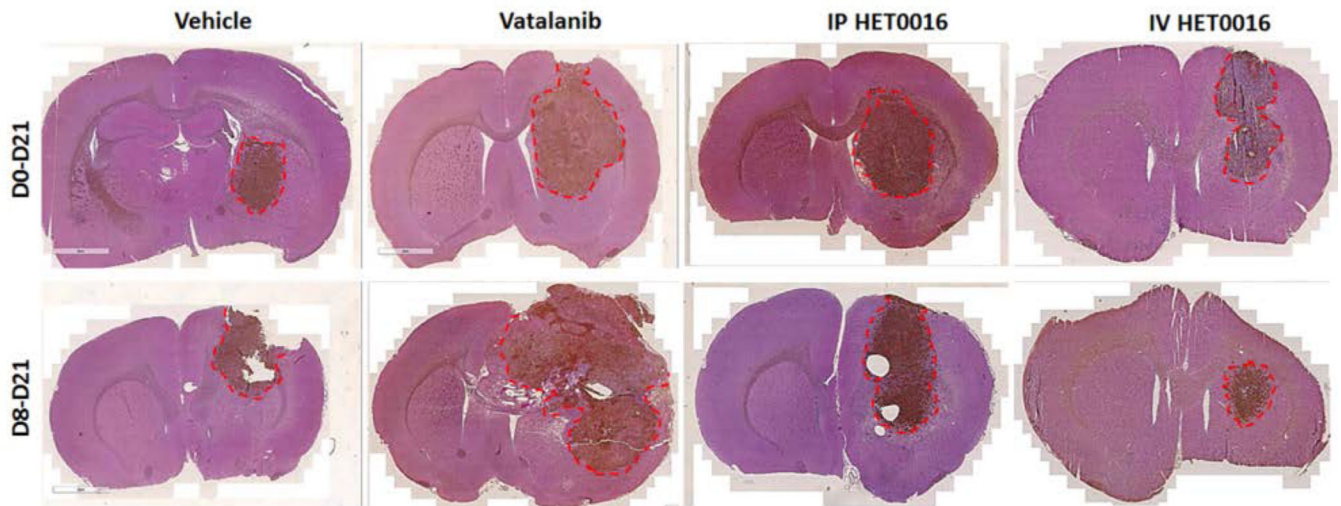


Figure 4. Vatalanib increased tumor growth and novel IV formulation of HET0016 decreased tumor growth of human GBM in rat model

Immunohistochemistry (MHC-1) images show tumor sizes following drug treatments compared to vehicle. Tumor size is distinguished by dotted line.

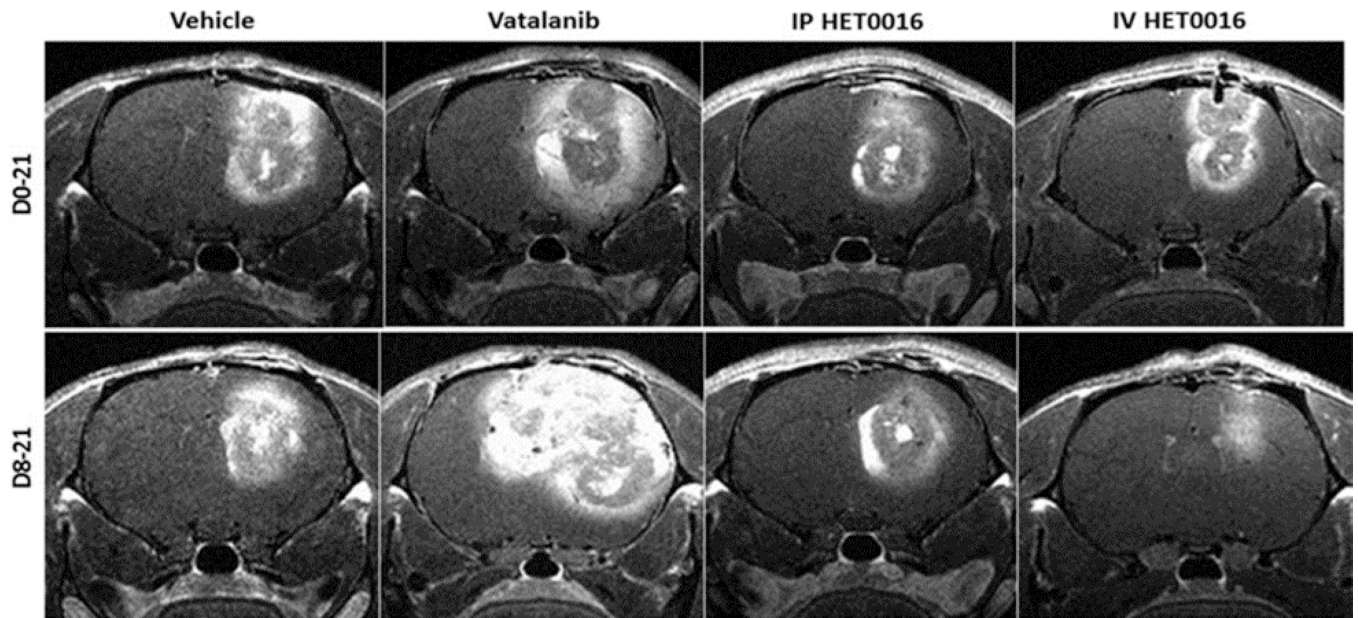


Figure 5. Vatalanib increased tumor growth and novel IV formulation of HET0016 decreased tumor growth of human GBM in rat model

T1 post contrast MRI images from corresponding animals show tumor size following drug treatments compared to vehicle.

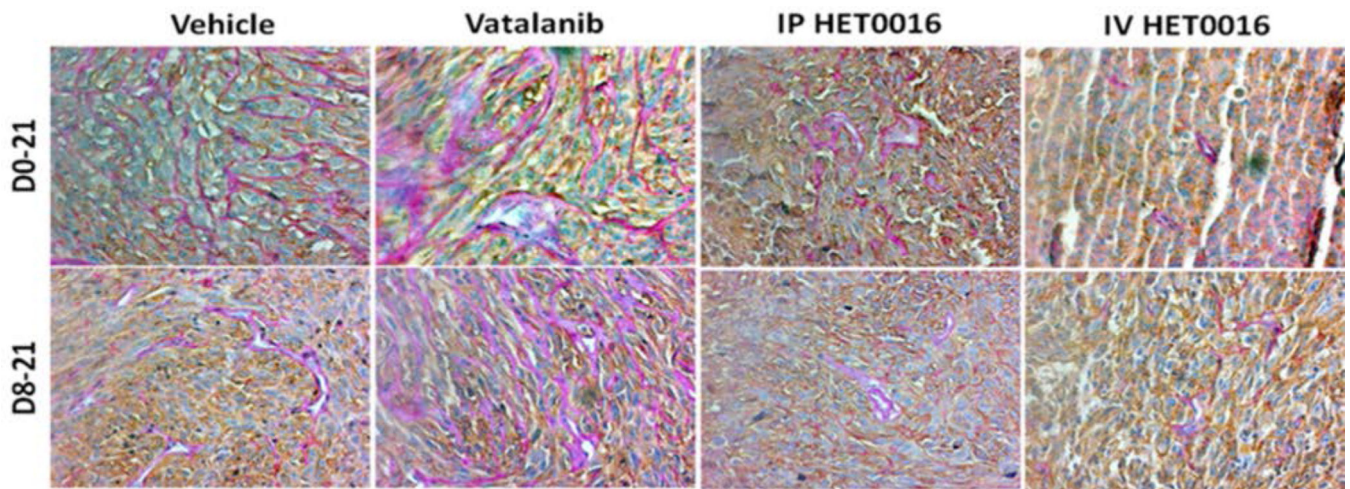


Figure 6. Vatalanib increased number of VM and novel IV formulation of HET0016 decreased VM of human GBM in rat model

(A) Immunohistochemistry data showing PAS stain representing increased VM (pink vessel-like strictures due to PAS+) in Vatalanib treated tumors compared to vehicle. VM was significantly decreased in HET0016 treated groups both IP and IV compared to vehicle or Vatalanib (less number of pink vessel-like structures). Brown cells are human marker MHC-1 positive cells (human U251 GBM cells). The pink vessel-like structures are lined by brown MHC-1 positive cells.

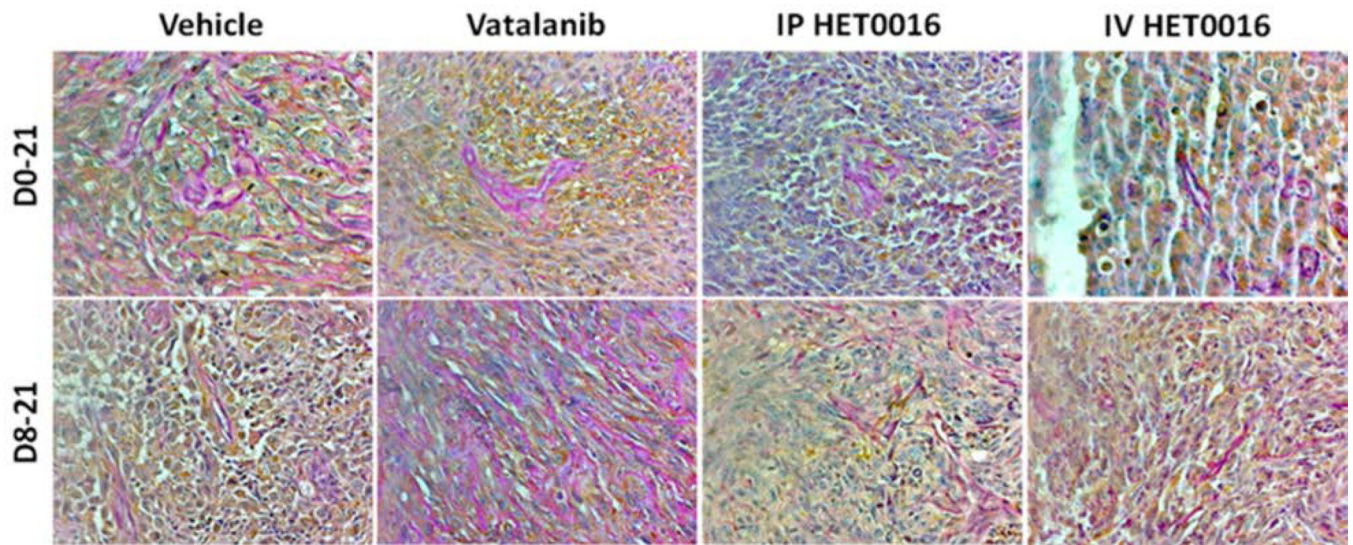


Figure 7. Vatalanib increased hypoxia and novel IV formulation of HET0016 decreased hypoxia in human GBM rat model

Immunohistochemistry data showing HIF1 α stain representing increased hypoxia in Vatalanib treated tumors compared to vehicle. HIF-1 α positive cells are low in HET0016 treated tumors. The images were taken from the consecutive sections of MHC-1 plus PAS positive areas shown in Figure 6 at the corresponding core of the tumors.

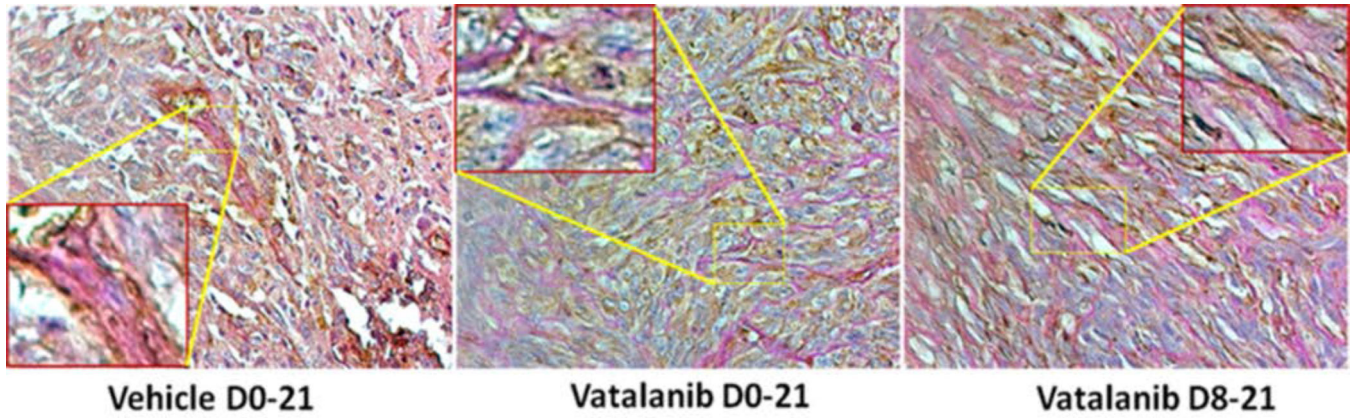


Figure 8. PAS+ areas also correspond to basal laminae of vascular structures (VM)
Consecutive sections were double stained for PAS and laminin to validate that PAS+ areas are not due to deposition of glycogen. Presence of both PAS and laminin indicate the vascular structures with functional basal laminae indicating VM (insets).

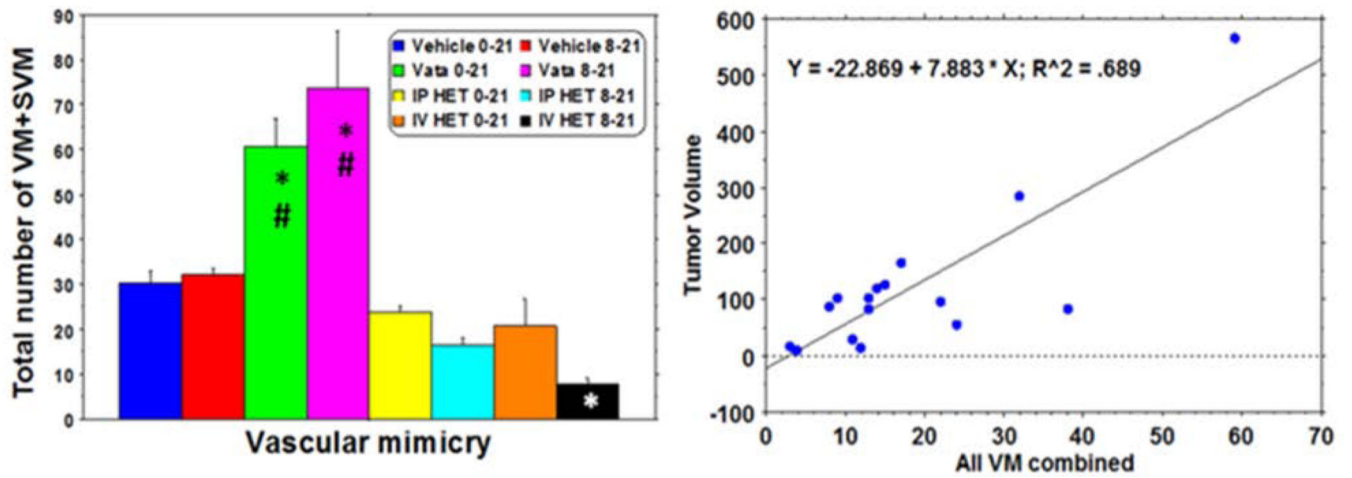


Figure 9. Evidence of AAT induced VM and its different stages in GBM tumor growth
 Quantitative evaluation of VM following treatments and its correlation with tumor growth.

Author Manuscript

Author Manuscript

Author Manuscript

Author Manuscript